Selection of control structure and temperature location for two-product distillation columns

Eduardo Shigueo Hori, Sigurd Skogestad*

Department of Chemical Engineering

Norwegian University of Science and Technology

N-7491 Trondheim, Norway

Abstract

The choice of control structures for distillation columns is important for practical industrial operation. There is no single "best" structure for all columns, so some authors feel that each column should be treated independently. Nevertheless, the objective of this work is to find a structure that is "reasonable" for all columns. In this paper, we consider the steady-state deviations in product compositions in response to disturbances, assuming that only flows and temperatures are available for control. For most columns a good choice is to fix reflux and a temperature. For binary separations, the temperature should be located where the temperature slope is steep. For multicomponent mixtures, the same rule applies except that one should avoid column sections with large changes in non-key component, for example at the column end and at the feed. Control of two temperatures is better for some columns, but not all.

Keywords: Distillation column, multicomponent distillation, control structure selection.

1. Introduction

Consider a conventional distillation column with a given feed and pressure controlled using cooling. The degrees of freedom are then the reflux, boilup, distillate and bottom flows, $\mathbf{u}_0 = \begin{bmatrix} L & V & D & B \end{bmatrix}$. To stabilize the column, liquid levels need to be controlled, and since the level set points have no steady-state effect, we are left with two steady-state degrees of freedom (Shinskey, 1984). For the further analysis in this paper it does not matter what these degrees of freedom are as long as they

* Corresponding author. E-mail: skoge@chemeng.ntnu.no; Fax: +47-7359-4080; Phone: +47-7359-4154

are independent at steady-state, so let us select them as $\mathbf{u} = \begin{bmatrix} L & V \end{bmatrix}$. For this study, the main assumptions are:

1. Consider steady state only.
2. Two-product column with given feed and fixed pressure.
3. Two-point product composition control is desired, but the composition measurements are not available (at least not for fast control).
4. Variables available for control: all temperatures and flows (including flow ratios L/D, L/F, etc.)
5. The objective function *J* for the indirect composition control problem is

$$\sqrt{J} = \Delta X = \sqrt{\left(\frac{x^{\mathrm{H}}_{\mathrm{top}} - x^{\mathrm{H}}_{\mathrm{top,s}}}{x^{\mathrm{H}}_{\mathrm{top,s}}}\right)^2 + \left(\frac{x^{\mathrm{L}}_{\mathrm{btm}} - x^{\mathrm{L}}_{\mathrm{btm,s}}}{x^{\mathrm{L}}_{\mathrm{btm,s}}}\right)^2} \tag{1}$$

where ΔX is the root mean square of the relative steady state composition deviation. Typically, ΔX should be of the order 1 or less. L and H denote the light and heavy key components, respectively.

The question is: What should we use the two degrees of freedom for, that is, what are the controlled variables c? Should reflux and a temperature be fixed, $\mathbf{c} = \begin{bmatrix} L & T \end{bmatrix}$, in order to minimize ΔX ? To analyze this we consider product composition variations in response to disturbances. Assuming constant stage efficiency any control structure which controls two intensive variables (e.g. L/D and V/B, or two temperatures) will have perfect disturbance rejection for feed flowrate disturbance. Therefore, as pointed out by Luyben (2005), the main disturbances to consider are in feed composition. In addition, the effect of implementation error should be considered (Skogestad, 2000).

Notation (see also separate): Instead of stage numbers, we use in the tables the relative distance (in percentage) from each end to the feed stage (see Figure 1):

- top section: $$\%\mathrm{top} = \frac{(N - N_i)}{(N - N_F)} * 100 \tag{2}$$

- bottom section: $$\%btm = \frac{(N_i - 1)}{(N_F - 1)} * 100 \tag{3}$$

Here N_i is the stage number counted from bottom, N_F is the feed stage and N is the total number of stages in the column.

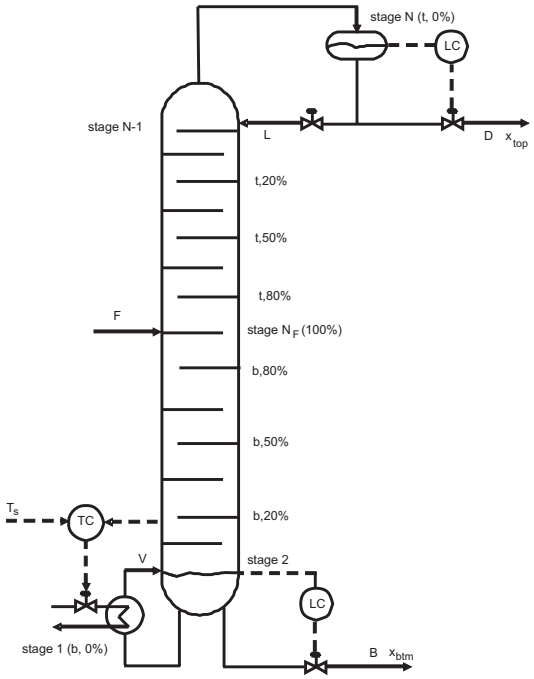

Figure 1. Distillation column with fixed reflux L and temperature control in the bottom section.

2. Methods for Evaluating Controlled Variables

The most common approach to achieve indirect composition control is to control temperature (Luyben, 2006). Some proposed rule for selecting temperature locations are

1. The temperature slope between two stages $\Delta T / \Delta N$ must be large (Luyben, 2005). As shown in the Appendix, this is reasonable for dynamic reasons.
2. Look for temperatures with a small optimal variation ($\Delta T_{opt} / \Delta F$, $\Delta T_{opt} / \Delta z_F$ and $\Delta T_{opt} / \Delta q_F$) in the selected variables (Luyben, 1975).
3. Look for variables (temperatures) with a large sensitivity $\Delta G = \Delta T / \Delta L$ (Tolliver and McCune, 1980) or, more generally, with a large minimum singular value ($\underline{\sigma}(\mathbf{G})$), from the inputs **u** to temperatures **c** (Moore, 1992).

The above rules are mostly empirical. For binary separations, rules 1 and 3 give the same result and favor locations where the temperature slope is large which is usually away from the column ends, whereas rule 2 favors locations close to the column ends. Skogestad (2000) showed that rules 2 and 3 can be combined rigorously into the "maximum gain rule" by using rule 2 as a scaling factor for rule 3. More precisely, one should maximize the minimum singular value of the scaled steady state gain matrix ($\underline{\sigma}(\mathbf{G}')$) from **u** to **c**. In the scalar case, we want to maximize:

$$\left|\mathbf{G}'\right| = \frac{\left|\mathrm{d}T/\mathrm{d}L\right|}{\left|\frac{\mathrm{d}T^{\mathrm{opt}}}{\mathrm{d}z_{\mathrm{F}}}\right|\Delta z_{\mathrm{F}} + \left|\frac{\mathrm{d}T^{\mathrm{opt}}}{\mathrm{d}F}\right|\Delta F + \left|\frac{\mathrm{d}T^{\mathrm{opt}}}{\mathrm{d}q_{\mathrm{F}}}\right|\Delta q_{\mathrm{F}} + \Delta T^{\mathrm{n}}} \tag{4}$$

where Δz_{F} , ΔF , and Δq_{F} are the expected (typical) disturbances and ΔT^{n} is the expected implementation/measurement error for controlling temperature.

However, also method is not exact, at least in the multivariable case. Thus, in this paper we mainly use the exact local method of Halvorsen et al. (2003) where it is shown that the worst-case steady-state composition deviation in Eq. (1) is given by:

$$\Delta X = \bar{\sigma}\left(\begin{bmatrix}\mathbf{M}_{\mathrm{d}} & \mathbf{M}_{\mathrm{n}}\end{bmatrix}\right)^2 \Big/ 2 \tag{5}$$

where

$$\mathbf{M}_{\mathrm{d}} = \mathbf{J}_{\mathrm{uu}}^{1/2}\left(\mathbf{J}_{\mathrm{uu}}^{-1}\mathbf{J}_{\mathrm{ud}} - \mathbf{G}^{-1}\mathbf{G}_{\mathrm{d}}\right)\mathbf{W}_{\mathrm{d}}\,,\ \mathbf{M}_{\mathrm{n}} = \mathbf{J}_{\mathrm{uu}}^{1/2}\mathbf{G}^{-1}\mathbf{W}_{\mathrm{n}} \tag{6}$$

The magnitude of the disturbances and implementation errors enter into the diagonal matrices $\mathbf{W}_{\mathrm{d}}$ and $\mathbf{W}_{\mathrm{n}}$. In this paper, the following expected disturbances are used: $\Delta F = \pm 20\%$, $\Delta z_F = \pm 10\%$, $\Delta q_F = \pm 10\%$. The implementation error for temperature is $\Delta T^n = \pm 0.5K$ and it is $\pm 10\%$ for flows and $\pm 15\%$ for flow ratios. The 2×2 steady-state gain matrices **G** and $\mathbf{G_d}$ are from the inputs $u = \begin{bmatrix}L & V\end{bmatrix}^{\mathrm{T}}$ to the two candidate controlled variables **c**, e.g. $c = \begin{bmatrix}T & L\end{bmatrix}$ if we fix T and L. They may be obtained numerically by applying small perturbations in the inputs **u**. In our case, $\mathbf{J_{uu}}$ and $\mathbf{J_{ud}}$ are given by

$$\mathbf{J}_{\mathrm{uu}} = 2\mathbf{G}_1^{\mathrm{T}}\mathbf{Q}\mathbf{G}_1 \quad \text{and} \quad \mathbf{J}_{\mathrm{ud}} = 2\mathbf{G}_1^{\mathrm{T}}\mathbf{Q}\mathbf{G}_{\mathrm{d1}} \tag{7}$$

Where $\mathbf{G}_1$ and $\mathbf{G}_{\mathrm{d1}}$ are the gain matrices from $u = \begin{bmatrix}L & V\end{bmatrix}^{\mathrm{T}}$ to $y_1 = \begin{bmatrix}x_{\mathrm{top}}^{\mathrm{H}} & x_{\mathrm{btm}}^{\mathrm{L}}\end{bmatrix}^{\mathrm{T}}$ and $\mathbf{Q} = \mathrm{diag}\left(\begin{bmatrix}1/\left(x_{\mathrm{top}}^{\mathrm{H}}\right)^2 & 1/\left(x_{\mathrm{btm}}^{\mathrm{L}}\right)^2\end{bmatrix}\right)$.

3. Binary Distillation Columns

The variable selection methods were applied to different binary and multicomponent distillation columns. The components are mostly “ideal” and denoted A (lightest), B, C and D (heaviest). The key components are denoted L for light and H for heavy. In this section we consider binary mixtures where L=A and H=B. Steady-state data for these columns are given in Table 1. Columns A-J are ideal with

constant relative volatility and columns M1-M6 are methanol-water columns (Luyben, 2005). The disturbances are the feed flow rate (F), feed enthalpy (q_F) and feed composition (z_F).

Table 1: Steady state data for binary distillation column examples (Skogestad et al., 1990)

Column	z_F^L	α	N	N_F (from btm)	x_{top}^H	x_{btm}^L	D/F	L/F	$T_{B,H}$[$]	$T_{B,L}$[$]
A	0.5	1.5	41	21	0.01	0.01	0.500	2.706	10	0
B	0.1	1.5	41	21	0.01	0.01	0.092	2.329	10	0
C	0.5	1.5	41	21	0.01	0.002	0.555	2.737	10	0
D	0.65	1.12	111	39	0.005	0.10	0.614	11.862	2.9	0
E	0.2	5	16	5	0.0001	0.05	0.158	0.226	40.9	0
F	0.5	15	11	5	0.0001	0.0001	0.500	0.227	68.7	0
G	0.5	1.5	81	40	0.0001	0.0001	0.500	2.635	10	0
H	0.27	1.36	93	40	0.02	0.02	0.260	2.663	7.8	0
I	0.9	1.5	41	21	0.0011	0.01	0.891	3.305	10	0
J	0.1	1.5	41	21	0.01	0.0011	0.109	3.314	10	0
M1*	0.1	-	42	30	0.001	0.001	0.099	0.408	-	-
M2*	0.2	-	37	24	0.001	0.001	0.199	0.404	-	-
M3*	0.4	-	32	17	0.001	0.001	0.400	0.404	-	-
M4*	0.6	-	32	14	0.001	0.001	0.600	0.386	-	-
M5*	0.8	-	37	13	0.001	0.001	0.801	0.366	-	-
M6*	0.9	-	32	12	0.001	0.001	0.901	0.357	-	-

Light key component (L), Heavy key component (H)
* Luyben's methanol-water columns (Luyben, 2005). These columns are simulated using ASPEN PLUS©
[$] Boiling point of light component set to 0 [°C], and the other adjusted to be compatible with relative volatility

For simplicity, the temperatures are assumed to depend linearly on liquid composition and calculated as (for columns A-J):

$$T_i = T_{B,H} x_i^H + T_{B,L} x_i^L \tag{8}$$

This assumption may seem very crude, but actually does not have much effect on the results.

3.1. Binary Column A

The first example of a binary separation is "column A" with a feed of 50% light component and 50% heavy component and relative volatility of 1.5. The column has 1% of heavy component in the top (and 99% lights) and 1% light component in the bottom. Figure 2 shows the temperature profile resulting from changes in reflux (L) with fixed V (left plot) and the resulting steady-state gains $\Delta T / \Delta L$ (dashed line in right plot). The plot indicates that the most sensitive locations are away from the column ends, but not close to the feed (at about 70% from the column ends). For illustration purposes, large values of ΔL are used in the left plot, but a small change is used when evaluating the gains in the right plot.

In Figure 3 is shown the nominal temperature profile (left) and its slope $\Delta T / \Delta N$ (right). We note that there is a very close agreement in the binary case between the gain $\Delta T / \Delta L$ (Figure 2) and the slope $\Delta T / \Delta N$ (Figure 3).

In Figure 4 is shown the optimal temperature profile resulting from a disturbance in feed composition z_F (left), and the resulting optimal variation $\Delta T^{opt} = \left| dT^{opt} / dd_i \right| \Delta d_i$ for disturbances (d_i) in F, z_F and q_F (right). The optimal variation in temperature is seen to depend mainly on z_F, and is large (undesired) at the middle of the column and small (zero) at the column ends. This favors locating the temperature measurement towards the column end. To make a trade-off between these conflicting results, the gain $\left| \Delta T / \Delta L \right|$ in Figure 2 (right) that favors locating the temperature towards the feed stage, and optimal variation (ΔT^{opt}) in Figure 3 (right), that favors locating the temperature close to the column ends, we plot in Figure 5 the scaled steady-state gain $\left| G' \right|$ in Eq. (4). The scaled gain is the ratio of $\Delta T / \Delta L$ (Figure 2) and ΔT^{opt} (Figure 3) + ΔT_j^n and we find as expected that the scaling moves the optimal location somewhere close to the column ends, but the effect of the scaling is small in this case.

A more exact approach, especially for the case when one wants to select two temperatures, is to consider the steady-state composition deviation ΔX given in Eq. (5). The results are summarized in Figure 6 which shows ΔX with 1) fixed L/F and T, 2) fixed V/F and T, and 3) two fixed symmetrically located temperatures (same % for top and bottom). The plot in Figure 6 agrees with the scaled gain in Figure 5 and shows that one should avoid temperatures located close to the column ends.

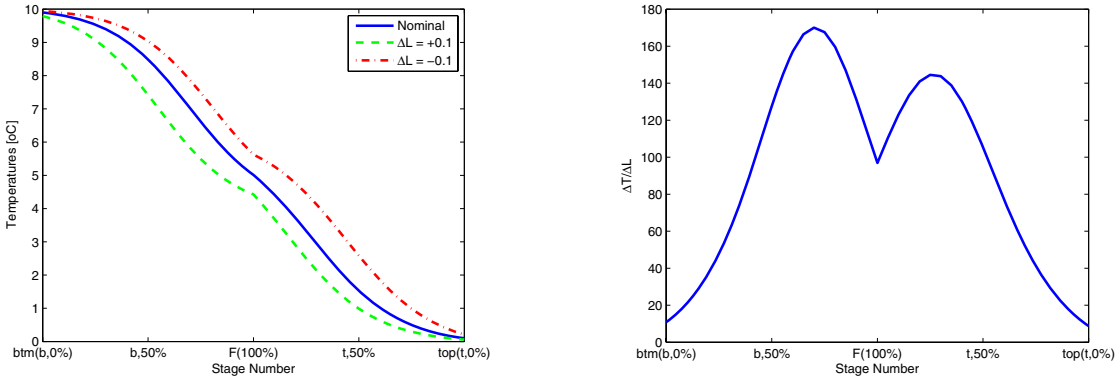

Figure 2. Binary column A: Temperature profile resulting from change in reflux (L) with fixed V (left) and resulting steady-state gain $\left| \Delta T / \Delta L \right|$ for small ΔL (right).

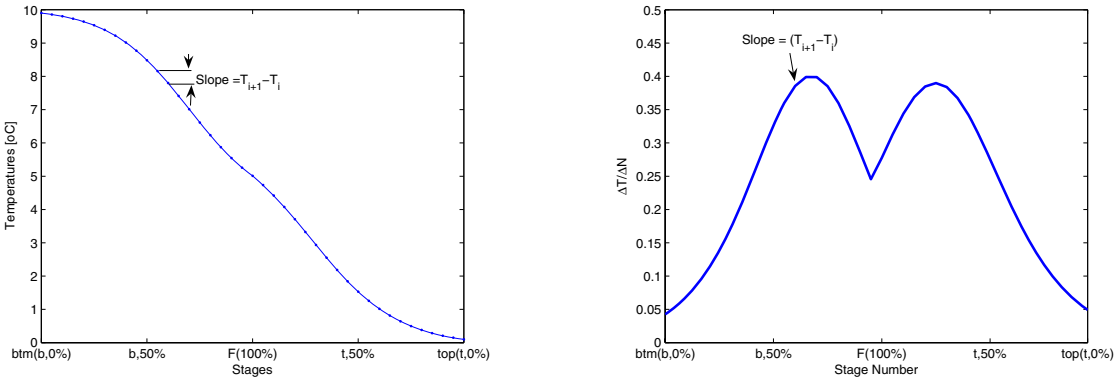

(a) (b)

Figure 3. Binary column A: (a) temperature profile, and (b) resulting temperature slope ($\Delta T / \Delta N$).

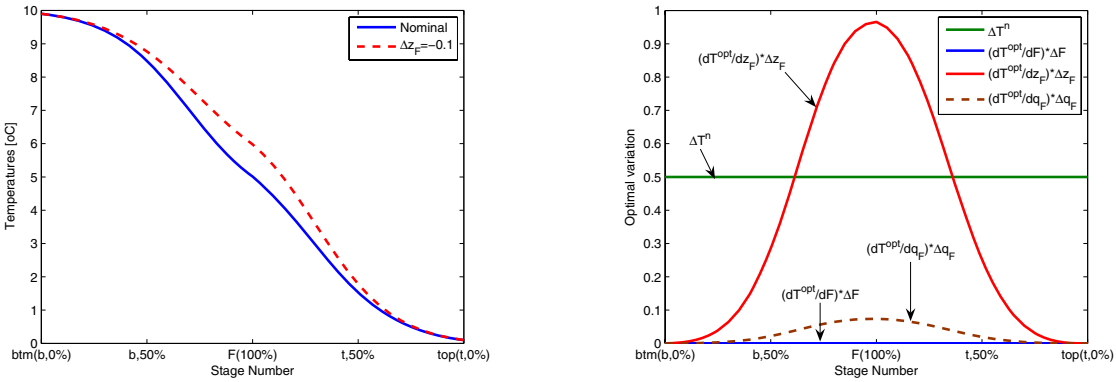

Figure 4. Binary column A: Re-optimized temperature profile for disturbance in z_F (left) and resulting optimal variation for the main disturbances (right).

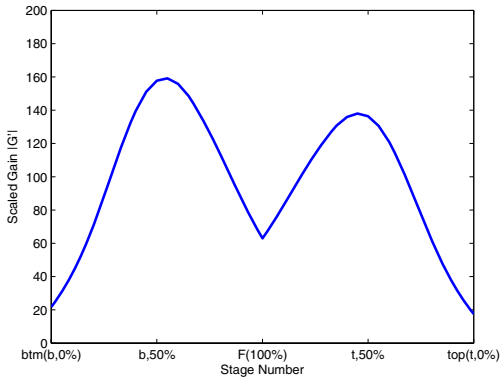

Figure 5. Binary column A: Scaled gain $\left|G'\right|$ computed from Eq. (4).

More detailed results for ΔX are shown in Table 2 for a large number of other control structures. Since there are many possible temperature locations, we show only results for (i) the temperature located in the middle of the section and (ii) for the optimal location (denoted *). Note that, for easy reference, we here put in boldface the combinations with L and L/F and the optimal temperatures.

For column A, the smallest steady state composition deviation (ΔX) of 0.530 is obtained when we control the two temperatures on stages 12 ($T_{b,55\%}$) and 30 ($T_{t,55\%}$), that is, with the temperatures symmetrically located on each side of the feed stage. The best combination of a flow and a temperature is to use L/F and a temperature in the bottom section ($T_{b,70\%}$), which has a composition deviation of 0.916, followed by V/F and $T_{b,75\%}$ with a deviation of 1.148.

However, if the purity of the top product is our primary concern, then it is usually better to fix a temperature in the top section. Also, fixing both a flow and a temperature in the same section (e.g. T_b-V/F) may give undesirable interactions if we later add a composition control layer (which uses the setpoints for V/F and T_b as manipulated variables). Therefore, we also show in the table the best combination with a temperature in the other section (denoted **). For example, with a fixed reflux to feed ratio L/F, the best temperature in the bottom section ($T_{b,70\%}$) gives $\Delta X = 0.916$ and best control of the bottom product ($\Delta X_{top} = 0.914$ and $\Delta X_{btm} = 0.588$). On the other hand, the best temperature in the top section ($T_{t,75\%}$) gives $\Delta X = 1.150$ and best control of the top product ($\Delta X_{top} = 0.588$ and $\Delta X_{btm} = 1.145$).

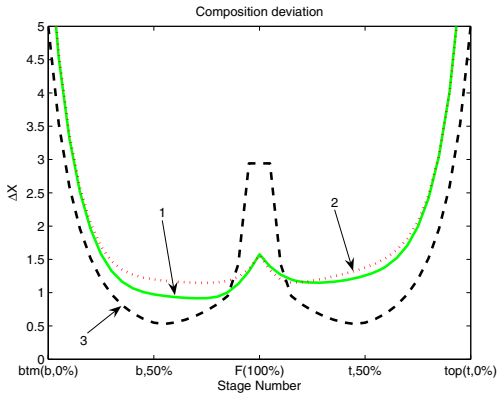

Figure 6. Binary column A: Composition deviation (ΔX) for fixing temperature at different locations: (1) L/F and one temperature. (2) V/F and one temperature. (3) Two symmetrically located temperatures.

Now consider structures without temperature control. The best combination with two fixed flows is L/D and V/B, with a deviation of 15.84 (Table 2). Keeping L and V constant gives a deviation of 63.42.

Perhaps surprisingly, the deviation with L/F and V/F constant is 50% larger. The reason is the implementation error, which is larger for ratios (15%) than for individual flows (10%); see section 2.

Several structures were compared by dynamic simulation (see Figure 7), confirming that the structure with fixed $T_{b,55\%}$-$T_{t,55\%}$ is the best. The levels are assumed to be tightly controlled using *D* and *B* (LV configuration for levels), and the remaining flows, $\mathbf{u} = \begin{bmatrix} L & V \end{bmatrix}$, were either fixed, used for temperature control or used to keep fixed ratios (L/F, V/F, L/D or V/B). The controllers were tuned using the SIMC rules (Skogestad, 2003), with $\tau_c \geq 1$ min and $\theta_m = 0$ (measurement delay).

Table 2: Steady-state relative composition deviations (ΔX) for alternative structures for binary column A.

Structure (Fixed variables)	ΔX_{top}	ΔX_{btm}	ΔX	**Structure (Fixed variables)**	ΔX_{top}	ΔX_{btm}	ΔX
$T_{b,55\%} - T_{t,55\%}$*	0.519	0.523	0.530	$T_{t,50\%} - V$	0.537	1.967	1.971
$T_{b,70\%} - L/F$*	0.914	0.588	0.916	$T_{t,50\%} - V/B$	0.635	2.040	2.071
$T_{b,50\%} - L/F$	0.971	0.509	0.975	$T_{t,95\%} - L/D$**	0.609	2.102	2.103
$T_{b,75\%}$ - V/F*	1.147	0.622	1.148	$T_{b,95\%} - V/B$**	2.178	0.706	2.181
$T_{t,85\%}$ - V/F**	0.849	1.148	1.152	$T_{t,50\%} - L/D$	0.431	2.327	2.327
$T_{t,75\%} - L/F$**	0.588	1.145	1.150	$T_{b,50\%} - V/B$	2.334	0.445	2.334
$T_{b,50\%}$ - V/F	1.197	0.499	1.199	L/D – V/B	9.805	12.46	15.84
$T_{b,90\%} - L$*	**1.223**	**1.072**	**1.223**	L/F – V/B	11.76	14.41	18.59
$T_{t,50\%} - L/F$	0.482	1.251	1.256	L – B	13.56	16.14	21.06
$T_{b,70\%} - L/D$*	1.145	0.830	1.321	D – V	12.61	17.09	21.22
$T_{t,50\%}$ - V/F	0.510	1.376	1.376	L/D – V	13.70	18.63	23.11
$T_{b,50\%} - L$	1.386	0.527	1.386	$T_{t,5\%} - B/F$*	3.367	25.05	25.05
$T_{b,50\%} - L/D$	1.358	0.606	1.393	$T_{t,5\%} - D/F$*	3.367	25.05	25.05
$T_{t,90\%} - L$**	0.957	1.447	1.447	$T_{t,5\%} - B$*	3.367	29.86	29.86
$T_{t,95\%} - V$*	1.281	1.464	1.470	$T_{t,5\%} - D$*	3.367	29.86	29.86
$T_{b,95\%} - V$**	1.474	1.240	1.474	L – V	39.24	49.83	63.42
$T_{b,50\%} - V$	1.683	0.524	1.684	L/F – V/F	55.98	70.52	90.03
$T_{t,85\%} - V/B$*	1.367	1.238	1.711	D – B	infeasible	infeasible	infeasible
$T_{t,50\%} - L$	0.505	1.734	1.734				

* Temperature optimally located
** Temperature optimally located in the other section

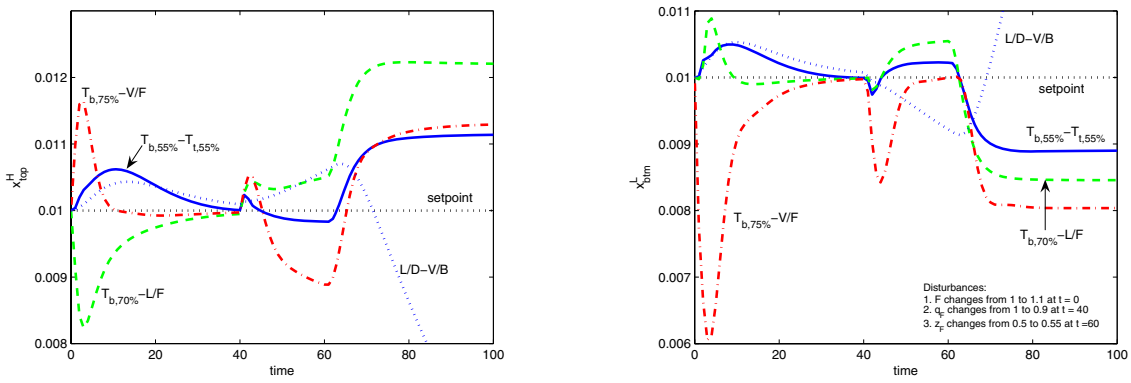

Figure 7. Dynamic composition response for alternative structure without explicit composition control (Binary Column A). Disturbances: F from 1 to 1.1 (t = 0); q_F from 1 to 0.9 (t = 40 min); and z_F from 0.5 to 0.55 (t = 60 min).

3.1.1. Addition of composition control layer

We here consider the case where a composition control layer is placed "on top" and adjusts the setpoints (for example, T_s and L_s) in the structures studied above. Typical dynamic simulations are shown in Figure 8 for a composition measurement delay $\theta_m = 10$ min. The results for varying delays θ_m are summarized in Table 3 by computing from the simulations the integrated squared error (ISE) for the top and bottom compositions.

$$ISE = \sqrt{\int \left(\frac{x - x_s}{x_s} \right)^2 dt} \tag{9}$$

The structures are listed in the same order as the "open loop" composition deviations in Table 2, so the results in Table 3 largely confirm that the best "self-optimizing" structures without composition control (Table 2) are best also with composition control (Table 3). This is especially the case for large measurement delays ($\theta_m = 60$ min), because then the composition layer becomes ineffective.

For smaller measurement delays we find, as expected, that the differences between the structures are smaller. For the shortest measurement delay ($\theta_m = 1$ min), the main surprise is the effectiveness of the L/D-V/B-structure (ISE_{sum} = 0.73). Note however that tight level control has been assumed and performance for this structure will deteriorate if the levels are detuned. Single loop controllers are used in the composition layer and it is found, as expected, that interactions give poor performance when there are two "manipulated variables" in the same section, eg. $T_{b,75\%}$-V/F (ISE_{sum} = 6.92) or $T_{t,50\%}$-L/F (ISE_{sum} = 3.82).

Table 3: With composition layer on top of lower layer control structures (Binary column A).

	$\theta_m = 1$ min			$\theta_m = 5$ min			$\theta_m = 10$ min			$\theta_m = 60$ min		
Lower-layer structure	ISE_{top}	ISE_{btm}	**Sum**	ISE_{top}	ISE_{btm}	**Sum**	ISE_{top}	ISE_{btm}	**Sum**	ISE_{top}	ISE_{btm}	**Sum**
$T_{b,55\%} - T_{t,55\%}$	0.60	0.58	**1.18**	1.61	1.55	**3.16**	2.26	2.23	**4.49**	5.28	5.37	**10.6**
$T_{b,70\%}$ – L/F	1.37	0.81	**2.18**	2.76	2.17	**4.93**	3.71	2.95	**6.66**	7.54	7.68	**15.2**
$T_{b,75\%}$ – V/F	2.94	3.98	**6.92**	4.27	5.04	**9.31**	5.39	5.14	**10.5**	11.9	8.99	**20.1**
$T_{t,85\%}$ - V/F	1.85	2.88	**4.73**	5.30	4.97	**10.3**	8.40	6.79	**15.2**	21.8	14.3	**36.1**
$T_{b,90\%}$ – L	1.11	1.22	**2.33**	3.70	3.58	**7.28**	6.88	5.78	**12.7**	22.8	17.3	**40.1**
$T_{t,50\%}$ - L/F	1.33	1.49	**3.82**	3.10	10.6	**13.7**	4.42	14.5	**18.9**	21.6	79.5	**101**
$T_{b,70\%}$ – L/D	0.73	0.62	**1.35**	2.66	2.12	**4.78**	4.39	3.45	**7.84**	13.1	9.95	**23.1**
$T_{t,95\%}$ – V	2.00	2.78	**4.78**	5.63	8.53	**14.2**	10.0	14.4	**24.4**	28.8	38.5	**67.3**
L/D – V/B	0.49	0.24	**0.73**	2.26	2.23	**4.48**	5.37	6.37	**11.8**	29.9	64.3	**94.2**
L -V	1.81	1.54	**3.35**	11.4	11.2	**22.6**	25.2	25.8	**51.0**	177	132	**309**

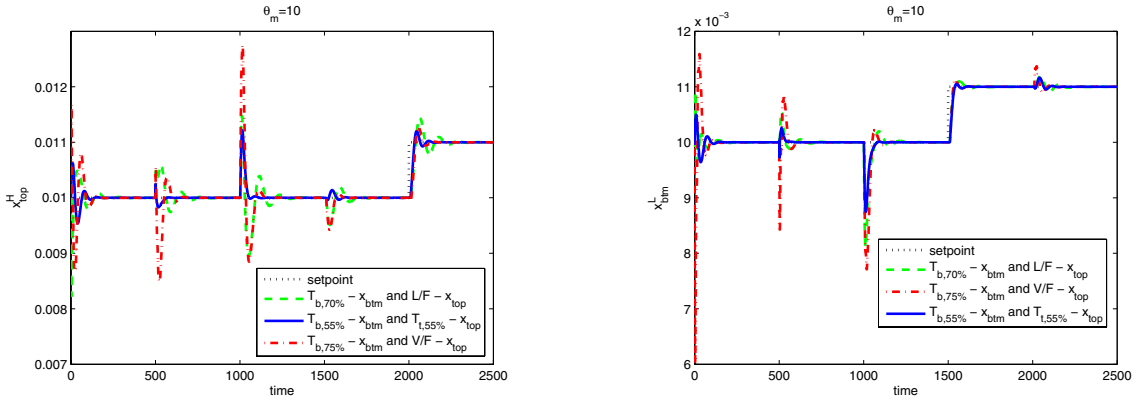

Figure 8. Dynamic response with composition layer ($\theta_m = 10$ min) – Binary column A. Disturbances: F from 1 to 1.1 (t = 0); q_F from 1 to 0.9 (t = 250); z_F from 0.5 to 0.55 (t = 500); $x^L_{btm,s}$ from 0.01 to 0.011 (t = 750); and $x^H_{top,s}$ from 0.01 to 0.011 (t = 1000).

3.2. Other ideal binary columns

The steady-state composition deviations (ΔX) without composition control for nine additional binary columns are summarized in Table 4. For about half of the columns it is best to fix two temperatures, but for the rest it is better to fix a flow and a temperature. If we want to keep a flow constant, a good structure in most cases is to keep L/F or L constant and fix a temperature.

Figure 9 shows the temperature profiles for all the ten binary columns. On the plots are also shown good temperature locations (indicated by cross) with fixed L or L/F. Figure 9 confirms that for binary columns a good rule is to locate the temperature where the temperature slope is large. The main exception seems to be column E, where the best location is in a fairly flat region towards the top.

Table 4: Binary mixtures steady-state composition deviations.

Column B	ΔX	**Column C**	ΔX	**Column D**	ΔX	**Column E**	ΔX
$T_{b,55\%}$-$T_{t,65\%}$*	0.783	**$T_{t,25\%}$ – L/F***	**0.700**	$T_{b,58\%}$ – L/D*	1.097	$T_{b,0\%}$-$T_{t,45\%}$*	0.745
$T_{t,65\%}$ – L/F*	**0.907**	$T_{t,45\%}$ – V/F*	0.703	$T_{b,50\%}$ – L/D	1.114	$T_{b,50\%}$-$T_{t,45\%}$	1.006
$T_{t,50\%}$ – L/F	0.934	$T_{t,50\%}$ – L/F	0.759	**$T_{b,50\%}$ – L/F***	**1.280**	**$T_{t,45\%}$ – L/F***	**1.032**
$T_{t,65\%}$ – V/F*	1.036	$T_{b,75\%}$ – $T_{t,35\%}$*	0.823	$T_{b,50\%}$ – V/F*	1.315	**$T_{t,36\%}$ - L***	**1.360**
$T_{t,50\%}$ – V/F	1.065	**$T_{t,50\%}$ - L***	**0.883**	**$T_{b,53\%}$ - L***	**1.444**	$T_{t,45\%}$ - L	1.388
$T_{t,75\%}$ - L*	**1.124**	$T_{b,85\%}$ – L/D*	0.918	$T_{b,55\%}$ - V*	1.496	$T_{t,36\%}$ – V/F*	1.580
$T_{t,50\%}$ - L	1.184	$T_{t,55\%}$ - V*	0.932	$T_{t,83\%}$ - V/F**	1.948	$T_{t,45\%}$ – V/F	1.644
$T_{t,75\%}$ - V*	1.239	$T_{t,50\%}$ - V	0.949	$T_{t,83\%}$ – V**	1.948	$T_{t,36\%}$ – V/B*	1.673
$T_{t,50\%}$ - V	1.299	$T_{t,5\%}$ – V/B*	1.201	$T_{t,78\%}$ – V/B*	2.025	$T_{t,45\%}$ – V/B	1.740
$T_{t,70\%}$ – V/B*	1.384	$T_{t,50\%}$ – L/D	1.238	$T_{b,50\%}$ – V/B	2.415	$T_{t,36\%}$ - V*	1.830
$T_{t,50\%}$ – V/B	1.426	$T_{b,80\%}$ – L/F**	1.534	$T_{b,29\%}$-$T_{t,72\%}$*	2.425	$T_{t,64\%}$ – L/F	1.835
$T_{b,70\%}$ – L/F**	2.706	$T_{t,50\%}$ – V/B	1.681	$T_{t,50\%}$ – V/B	3.345	$T_{t,45\%}$ - V	1.890
$T_{b,65\%}$ – L**	2.767	$T_{b,80\%}$ – L**	1.810	$T_{t,50\%}$ – V/F	3.649	$T_{b,75\%}$ – L/D*	4.860
$T_{b,50\%}$ – L/F	2.88	L/D – V/B	2.192	$T_{t,50\%}$ - V	3.662	$T_{b,0\%}$ – L/F**	5.623
$T_{b,50\%}$ – L	3.003	$T_{b,50\%}$ – L/D	2.232	$T_{t,50\%}$ – L/F	3.665	$T_{t,45\%}$ – L/D	5.639
$T_{b,50\%}$ – V/F	3.071	L/F – V/B	2.389	$T_{t,50\%}$ - L	3.677	$T_{b,50\%}$ – L/D	5.947
$T_{b,50\%}$ - V	3.205	L – B	2.767	L/D – V/B	3.854	$T_{b,50\%}$ – L/F	7.145
$T_{b,50\%}$ – V/B	3.627	$T_{b,50\%}$ – L/F	3.006	$T_{t,50\%}$ – L/D	4.248	$T_{b,0\%}$ – L**	8.075
$T_{b,25\%}$ – L/D*	5.485	$T_{b,50\%}$ – L	3.129	L/F – V/B	4.485	$T_{b,50\%}$ – L	8.766
$T_{b,50\%}$ – L/D	6.167	D – V	3.411	L – B	4.850	L/D – V/B	10.68
$T_{t,50\%}$ – L/D	7.961	$T_{b,50\%}$ – V/F	3.423	D – V	5.233	L/D – V	11.14
L/D – V/B	19.09	$T_{b,50\%}$ - V	3.646	L/D – V	5.852	D – V	12.43
D – V	19.10	L/D – V	3.735	L – V	56.04	$T_{b,50\%}$ – V/F	14.02
L/D – V	19.23	L – V	8.941	L/F - V/F	83.75	$T_{b,50\%}$ - V	15.60
L/F – V/B	33.64	L/F - V/F	12.49			$T_{b,50\%}$ – V/B	16.12
L – B	44.68	$T_{b,50\%}$ – V/B	24.75			L/F – V/B	16.73
L – V	71.09					L – V	19.40
L/F - V/F	102.1					L/F - V/F	20.98
						L – B	31.94

* Temperature optimally located

** Temperature optimally located in the other section

Table 4 (continued): Binary mixtures steady-state composition deviations.

Column F	ΔX	**Column G**	ΔX	**Column H**	ΔX	**Column I**	ΔX	**Column J**	ΔX
$T_{b,0\%}$–$T_{t,67\%}$*	0.763	$T_{b,64\%}$-$T_{t,68\%}$*	1.239	$T_{b,33\%}$-$T_{t,13\%}$*	0.878	**$T_{b,30\%}$ – L/F***	**0.932**	**$T_{t,35\%}$ – L/F***	**0.875**
$T_{t,83\%}$ - L*	**0.885**	**$T_{b,79\%}$ – L/F***	**1.904**	**$T_{t,34\%}$ – L/F***	**1.636**	$T_{b,35\%}$ – V/F*	0.955	$T_{t,50\%}$ – L/F	0.905
$T_{t,50\%}$ - L	1.005	$T_{t,93\%}$ – V/F*	2.068	$T_{t,23\%}$-V/F*	1.772	$T_{b,50\%}$ – L/F	0.988	$T_{t,35\%}$ – V/F*	0.986
$T_{b,75\%}$ – L/F*	**1.028**	**$T_{b,97\%}$ - L***	**2.520**	$T_{t,4\%}$-V/B*	2.227	$T_{b,50\%}$ – V/F	0.990	$T_{t,50\%}$ – V/F	1.019
$T_{b,75\%}$ – L**	1.124	$T_{b,77\%}$ – L/D*	2.602	**$T_{t,38\%}$-L***	**2.409**	**$T_{b,35\%}$ - L***	**1.133**	**$T_{t,40\%}$ - L***	**1.118**
$T_{t,50\%}$ – L/F	1.247	$T_{t,98\%}$ - V*	2.946	$T_{t,49\%}$-L/F	2.417	$T_{b,50\%}$ – L	1.162	$T_{t,50\%}$ - L	1.128
$T_{b,50\%}$ – L/F	1.497	$T_{b,51\%}$ – L/F	3.009	$T_{t,28\%}$-V*	2.549	$T_{b,40\%}$ – V*	1.257	$T_{t,40\%}$ - V*	1.221
$T_{b,50\%}$ – L/D*	1.530	$T_{b,51\%}$-$T_{t,51\%}$	3.099	$T_{t,49\%}$-L	2.582	$T_{b,50\%}$ - V	1.268	$T_{t,50\%}$ - V	1.235
$T_{b,50\%}$ – L	1.643	$T_{b,51\%}$ – L/D	3.127	$T_{t,49\%}$-V/F	2.587	$T_{b,25\%}$ – L/D*	1.339	$T_{t,30\%}$ – V/B*	1.433
$T_{b,50\%}$–$T_{t,50\%}$	1.886	$T_{b,51\%}$ – V/F	3.241	$T_{t,49\%}$-V	2.870	$T_{b,50\%}$ – L/D	1.403	$T_{t,50\%}$ – V/B	1.476
$T_{t,50\%}$ – L/D	1.946	$T_{b,51\%}$ – L	3.394	$T_{t,49\%}$-V/B	3.314	$T_{b,0\%}$–$T_{t,75\%}$*	3.617	$T_{t,40\%}$ – L/D	3.910
$T_{t,83\%}$ – V/F*	4.436	$T_{t,88\%}$ – V/B*	3.691	$T_{b,95\%}$-L/D*	8.837	$T_{b,40\%}$ – V/B*	4.718	$T_{t,50\%}$ – L/D*	3.911
$T_{b,50\%}$ – V/F	4.691	$T_{b,51\%}$ - V	3.858	$T_{t,58\%}$-L/D	11.71	$T_{b,50\%}$ – V/B	4.718	$T_{b,80\%}$-$T_{t,5\%}$*	3.915
$T_{t,50\%}$ – V/F	4.998	$T_{t,51\%}$ – L/F	4.005	$T_{b,51\%}$-L/D	12.38	$T_{t,90\%}$ – V/B*	5.086	$T_{b,95\%}$ – L/D**	5.271
$T_{t,83\%}$ – V*	5.014	$T_{t,51\%}$ – V/F	4.122	L/D-V/B	15.14	L/D – V/B	10.34	L/D – V/B	10.4
$T_{b,50\%}$ - V	5.421	$T_{t,51\%}$ - L	4.505	$T_{b,31\%}$-L/F	17.28	L/F – V/B	10.37	D – V	10.5
$T_{t,50\%}$ - V	5.638	$T_{b,51\%}$ – V/B	4.846	$T_{b,51\%}$-L/F	18.86	L – B	10.45	L/D – V	10.6
$T_{t,83\%}$ – V/B*	7.223	$T_{t,51\%}$ - V	4.868	$T_{b,31\%}$-L**	23.65	$T_{t,50\%}$ – V/B	10.52	$T_{b,50}$ – L/D	12.2
$T_{b,50\%}$ – V/B	7.620	$T_{t,51}$ – L/D	5.060	$T_{b,51\%}$-L	24.79	$T_{t,95\%}$ – V/F**	17.52	$T_{b,95\%}$ – L/F**	14.97
$T_{t,50\%}$ – V/B	8.130	$T_{t,51\%}$ – V/B	5.226	$T_{b,51\%}$-V/F	27.87	$T_{t,95\%}$ – V**	17.72	$T_{b,95\%}$ – L**	15.11
L/D – V/B	1600	L/D – V/B	1593	$T_{b,51\%}$-V	35.52	D – V	21.02	L/F – V/B	17.13
L/F – V/B	1667	L/F – V/B	1878	$T_{b,51\%}$-V/B	1636	L/D – V	23.24	L – B	21.03
L – B	2127	L – B	2140			$T_{t,50\%}$ – V/F	35.42	$T_{b,50\%}$ – L/F	34.70
D – V	2127	D – V	2141			$T_{t,50\%}$ - V	35.83	$T_{b,50\%}$ – L	34.90
L/D – V	2363	L/D – V	2333			$T_{t,50\%}$ – L/F	38.72	$T_{b,50\%}$ – V/F	37.66
L/F - V/F	2576	L – V	6344			$T_{t,50\%}$ - L	38.99	$T_{b,50\%}$ - V	37.89
L – V	2683	L/F - V/F	8993			L – V	53.79	L – V	46.18
						$T_{t,50\%}$ – L/D	60.09	$T_{b,50\%}$ – V/B	55.77
						L/F - V/F	75.26	L/F - V/F	67.48

* Temperature optimally located

** Temperature optimally located in the other section

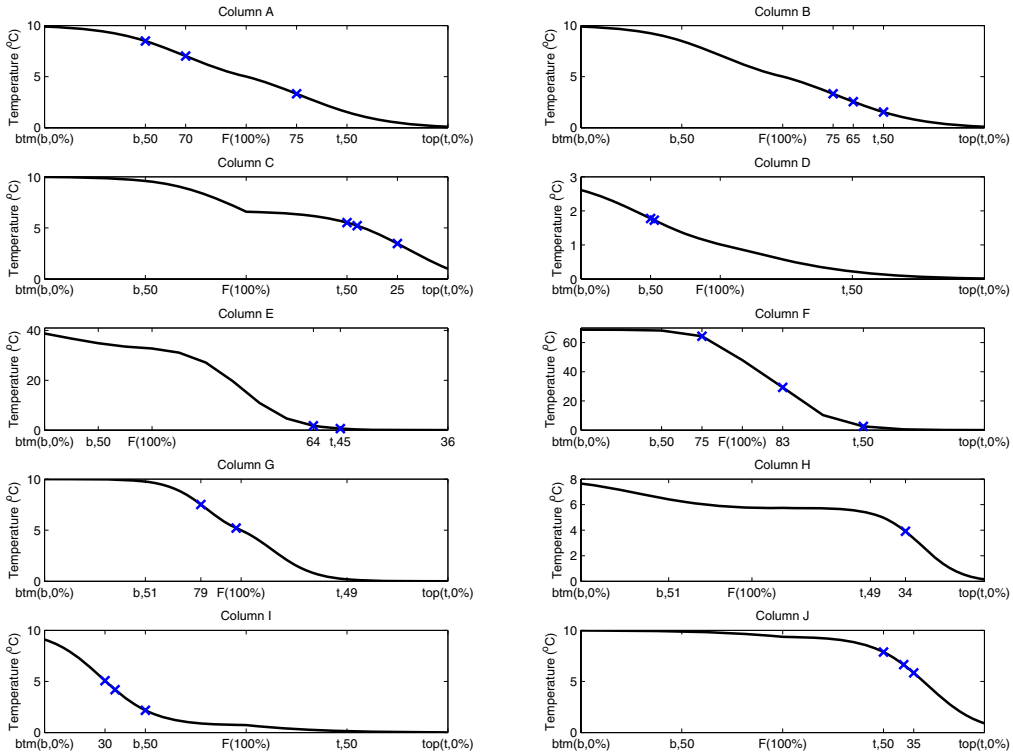

Figure 9. Temperature profiles for binary columns A-J with crosses to indicate good temperature locations with fixed L or L/F.

3.3. Binary methanol/water columns

In this section we consider the binary methanol/water columns M1-M6 studied by Luyben (2005). All columns have the same product purity (99.9%), but the feed composition varies in the range from 0.1 to 0.9 and the columns have been redesigned with respect to number of stages and feed location for each feed (see Table 1). The columns are simulated in ASPEN©, with flows fixed on a molar basis (which seems rather unrealistic for a liquid flow, but we here follow Luyben, and it is of minor importance because of the high-purity product). The disturbances considered in these columns are feed flow rate (F) and feed composition (z_F). Luyben studied the effect of feed compositions in the control structures and concluded that two-point temperature control is required for intermediate feed compositions, while single temperature control is adequate for low and high feed compositions. Our results in Table 5 confirm these findings. We note that controlling two temperatures gives a large improvement in most cases (in contrast to the results

for the ideal binary columns in Table 4), and we find that with only one temperature it is good to fix L or L/F (in agreement with the results in Table 4).

Figure 10 shows the temperature profiles for the columns along with good temperature locations for each column (cross) with fixed L or L/F. The plots confirm the rule for binary columns of locating the temperature measurement where the slope is large.

Table 5: Binary methanol-water columns (Luyben 2005): Steady-state composition deviations (ΔX).

Column M1	ΔX	**Column M2**	ΔX	**Column M3**	ΔX
$T_{b,10\%}$-$T_{t,17\%}$*	2.286	$T_{b,39\%}$–$T_{t,23\%}$*	1.356	$T_{b,19\%}$-$T_{t,27\%}$*	1.452
$T_{b,48\%}$-$T_{t,50\%}$	3.820	$T_{b,48\%}$–$T_{t,54\%}$	3.564	$T_{b,50\%}$-$T_{t,53\%}$$^{\$}$	2.945
$T_{t,17\%}$ – L/F*	**4.070**	**$T_{t,23\%}$ – L/F***	**8.615**	**$T_{b,19\%}$ – L/F***	**4.647**
$T_{t,50\%}$ – L/F$^{\$}$	4.555	$T_{t,46\%}$ – L/F$^{\$}$	8.670	$T_{b,50\%}$ – L/F$^{\$}$	4.845
$T_{t,17\%}$ - L*	**4.835**	**$T_{t,23\%}$ - L***	**9.254**	**$T_{b,50\%}$ - L***	**7.157**
$T_{t,50\%}$ - L	5.094	$T_{t,54\%}$ - L	9.467	$T_{b,69\%}$ – V/F*	8.995
$T_{t,8\%}$ – V/F*	8.412	$T_{t,23\%}$ – V/F*	18.01	$T_{b,50\%}$ – V/F	9.072
$T_{t,50\%}$ – V/F	9.442	$T_{t,54\%}$ – V/F	18.25	$T_{b,19\%}$ – L/D	9.279
$T_{t,8\%}$ - V*	9.738	$T_{t,23\%}$ – V	20.19	$T_{b,50}$ – L/D*	9.723
$T_{t,50\%}$ - V	10.55	$T_{t,54\%}$ - V*	20.42	$T_{b,69\%}$ - V*	14.08
$T_{t,8\%}$ – V/B*	11.43	$T_{t,85\%}$ – L/D*	23.31	$T_{b,50\%}$ - V	14.20
$T_{t,50\%}$ – V/B	12.59	$T_{t,54\%}$ – L/D	23.94	$T_{b,81\%}$– V/B*	15.31
$T_{t,50\%}$ – L/D*$^{\$}$	33.16	$T_{t,15\%}$ – V/B*	24.22	$T_{b,50\%}$ – V/B	15.63
$T_{b,24\%}$–L/F**	144.1	$T_{t,54\%}$ – V/B	24.56	$T_{t,53\%}$ – L/F	34.95
$T_{b,48\%}$ – L/F	149.9	$T_{b,65\%}$ – L/F**	75.05	$T_{t,20\%}$ – V/F**	37.87
$T_{b,97\%}$ – L/D	169.9	$T_{b,48\%}$ – L/F	76.23	$T_{t,53\%}$ - L	49.35
$T_{b,21\%}$ – L**	171.8	$T_{b,96\%}$ – L/D**	79.55	$T_{t,20\%}$– V/B**	50.82
$T_{b,48\%}$ – L	185.8	$T_{b,13\%}$ – L**	81.07	$T_{t,53\%}$ – V/F	56.72
$T_{b,59\%}$ – L/D$^{\$}$	434.0	$T_{b,48\%}$ – L	87.53	$T_{t,20\%}$ – V**	59.01
$T_{b,48\%}$ – L/D	439.5	$T_{b,48\%}$ – L/D	128.3	$T_{t,53\%}$ – V/B	69.28
$T_{b,48\%}$ – V/F	636.4	$T_{b,48\%}$ – V/F	274.2	$T_{t,53\%}$ - V	84.17
$T_{b,48\%}$ - V	734.0	$T_{b,48\%}$ - V	315.8	$T_{t,53\%}$ – L/D	105.4
$T_{b,51\%}$ – V/B	1241	$T_{b,48\%}$ – V/B	579.6		

* Temperature optimally located
** Temperature optimally located in the other section
$^{\$}$ Configuration studied by Luyben (2005)

Table 5 (continued): Binary mixtures (Luyben 2005): steady-state composition deviations.

Column M4	ΔX	**Column M5**	ΔX	**Column M6**	ΔX
$T_{b,23\%}$–$T_{t,22\%}$*	1.186	$T_{b,25\%}$-$T_{t,29\%}$*	0.958	$T_{b,18\%}$-$T_{t,30\%}$*	1.621
$T_{b,46\%}$–$T_{t,56\%}$$	1.535	$T_{b,50\%}$-$T_{t,50\%}$	2.000	**$T_{b,45\%}$ – L/F*$**	**2.116**
$T_{b,15\%}$ – L/F*	**4.670**	**$T_{b,25\%}$ – L/F***	**3.851**	$T_{b,45\%}$-$T_{t,50\%}$	2.934
$T_{b,46\%}$ – L/F$	4.715	$T_{b,50\%}$ – L/F$	3.855	**$T_{b,9\%}$ - L***	**3.212**
$T_{b,23\%}$- L*	**6.759**	$T_{b,8\%}$ – L/D*	5.132	$T_{b,9\%}$– L/D*	3.275
$T_{b,46\%}$ – L	6.764	$T_{b,50}$ – L/D	5.236	$T_{b,45\%}$ – L/D	3.288
$T_{b,8\%}$ – L/D*	7.719	**$T_{b,33\%}$- L***	**5.623**	$T_{b,45\%}$ – L	3.353
$T_{b,46\%}$ – L/D	7.847	$T_{b,50\%}$ – L	5.624	$T_{b,0\%}$ - V/F*	8.025
$T_{b,38\%}$ – V/F*	13.48	$T_{b,25\%}$ – V/F*	15.43	$T_{b,45\%}$ – V/F	8.497
$T_{b,46\%}$ – V/F	13.49	$T_{b,50\%}$ – V/F	15.44	$T_{b,18\%}$ - V*	8.544
$T_{b,77\%}$ - V*	19.42	$T_{b,25\%}$ – V*	21.75	$T_{b,45\%}$ - V	8.573
$T_{b,46\%}$ - V	19.43	$T_{b,50\%}$ - V	21.75	$T_{b,0\%}$ – V/B*	116.7
$T_{b,38\%}$ – V/B*	32.79	$T_{b,92\%}$ – V/B*	88.72	$T_{b,45\%}$ – V/B	123.1
$T_{b,46\%}$ – V/B	32.82	$T_{b,50\%}$ – V/B	88.98	$T_{t,50\%}$ – L/F	155.8
$T_{t,50\%}$ – L/F	68.17	$T_{t,50\%}$ – L/F	182.5	$T_{t,90\%}$ – V/F**	196.7
$T_{t,94\%}$ – V/F**	91.87	$T_{t,50\%}$ - L	256.2	$T_{t,50\%}$ - L	215.6
$T_{t,50\%}$ - L	95.30	$T_{t,50}$ – L/D	371.8	$T_{t,45\%}$ – L/D	235.0
$T_{t,50\%}$ – V/F	158.7	$T_{t,50\%}$ – V/B	514.0	$T_{t,95\%}$ – V**	251.2
$T_{t,50}$ – L/D	158.7	$T_{t,50\%}$ – V/F**	1081	$T_{t,95\%}$ – V/B**	416.2
$T_{t,94\%}$ – V/B**	106.1	$T_{t,50\%}$ – V**	1555	$T_{t,50\%}$ – V/F	529.4
$T_{t,50\%}$ – V/B	169.5			$T_{t,50\%}$ - V	659.8
$T_{t,28\%}$ – V**	206.7			$T_{t,50\%}$ – V/B	1096
$T_{t,50\%}$ - V	228.7				

* Temperature optimally located
** Temperature optimally located in the other section
$ Configuration studied by Luyben (2005)

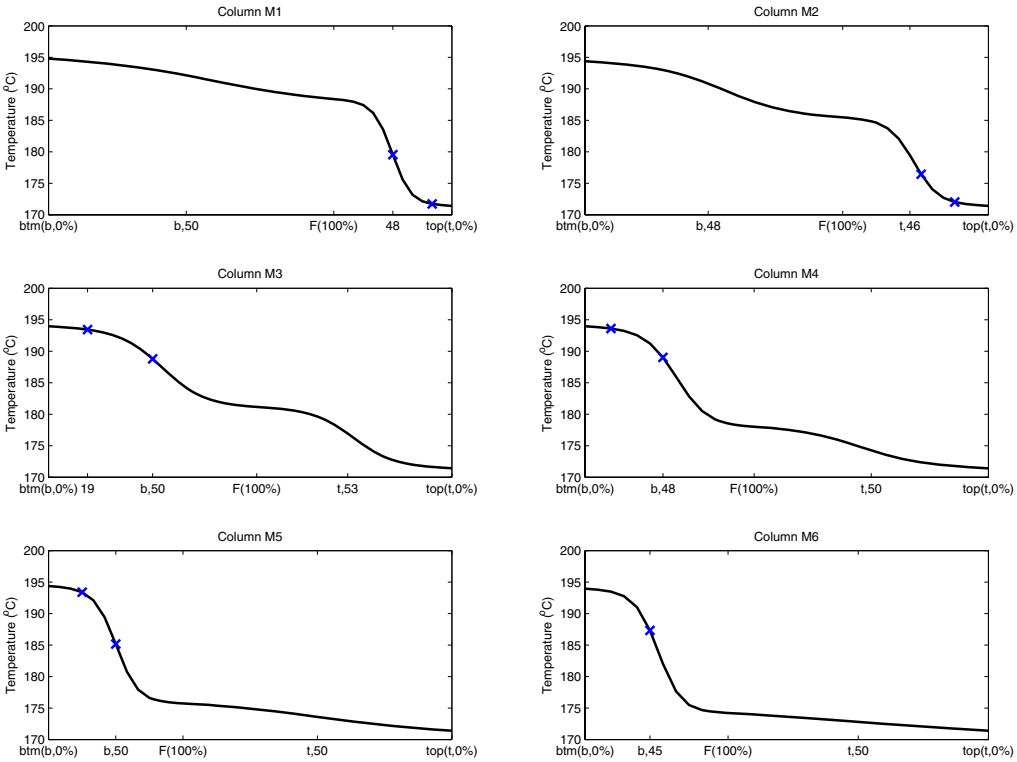

Figure 10. Temperature profiles for binary columns M1-M6 with cross to indicate good temperature locations with fixed L or L/F.

4. Multicomponent Distillation Columns

We here consider multicomponent extensions of column A. The feed has 25% of each component (A, B, C, D) and all relative volatilities are equal to 1.5 ($\alpha_{AB} = \alpha_{BC} = \alpha_{CD} = 1.5$). We consider three cases of splits L/H between light (L) and heavy (H) key components: A/B, B/C and C/D. The steady state column data is shown in Table 6 and the "temperatures" [°C] are calculated as:

$$T_i = 0x_{A,i} + 10x_{B,i} + 20x_{C,i} + 30x_{D,i} \tag{10}$$

In all cases, we have high purity separations on both ends with 1% or less of the key-component impurity.

Table 6: Multicomponent column data (extension of column A).

Key components (L/H)	N	N_F	x^H_{top}	x^L_{btm}	D/F	L/F
A/B	41	21	0.01	0.0033	0.250	2.767
B/C	41	21	0.005	0.005	0.500	1.659
C/D	41	21	0.0033	0.01	0.750	2.543
Depropanizer*	45	31	0.005	0.005	0.344	1.185

* Depropanizer feed composition (in mass fractions): 0.001 (C_2), 0.345 (C_3), 0.068 (i-C_4), 0.219 (n-C_4), 0.085 (i-C_5), 0.123 (n-C_5), and 0.159 (n-C_6).

4.1. B/C separation

We first consider the multicomponent separation between B and C (key components). This represents the most direct extension of the binary separation in "column A", by adding both a light (A) and heavy (D) non-key components. The composition profile is shown in Figure 11.

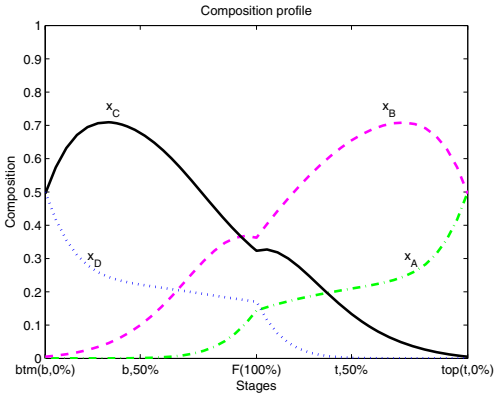

Figure 11. Steady state composition profile for B/C separation in multicomponent column A.

Figure 12 shows the temperature profile resulting from changes in reflux (L) with fixed V together with the resulting steady-state gain $\Delta T_i / \Delta L$ (right plot). The plot is very similar to the one for the binary case (Figure 2) and indicates that the temperature should be controlled away from the column ends, but not too close to the feed.

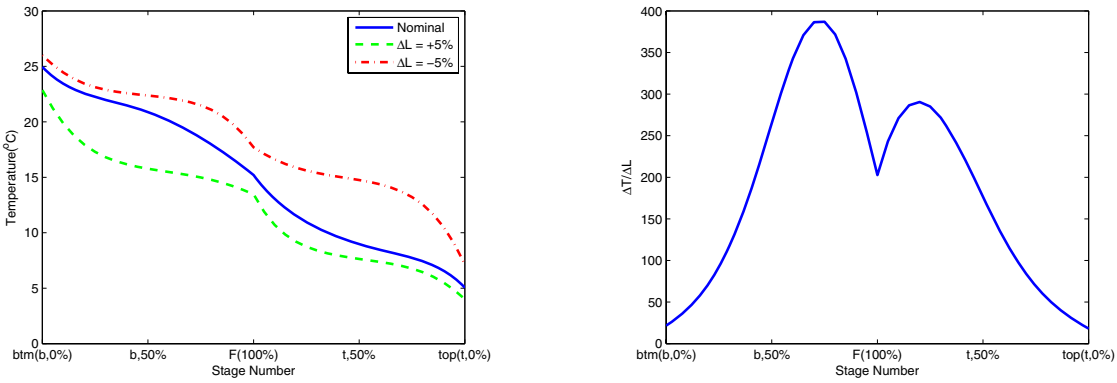

Figure 12. Temperature profile resulting from change in reflux (L) with fixed V and resulting steady-state gain ($\Delta T_i / \Delta L$) (multicomponent B/C separation).

However, in contrast to the binary case, the temperature slope $\Delta T / \Delta N$ (Figure 13) is almost the opposite of the gain $\Delta T_i / \Delta L$ (Figure 12). In particular, note that the slope $\Delta T / \Delta N$ is large towards the column ends, but this location should be avoided due to the small steady-state gain $\Delta T_i / \Delta L$ (Figure 12). Also note from Eq. (10) and Figure 11 that the temperature at the column ends depends strongly on the non-key components. Thus, temperature at the column end is not a good measure of the separation between the key components.

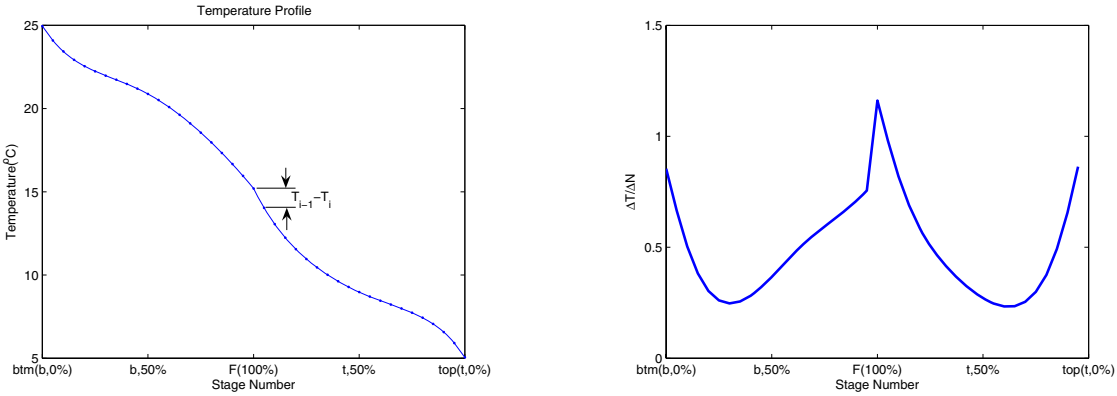

Figure 13. Nominal optimal temperature profile and resulted temperature slope $\Delta T / \Delta N$ for multicomponent B/C separation.

The optimal variation ΔT^{opt} for various disturbances is shown in Figure 14. Note that the optimal variation to a disturbance in z_F is large (undesirable) at the column ends, which is different from the binary case (Figure 4). The scaled gain $|G'|$ in Eq. (4) plotted in Figure 15 confirms that the column ends should

be avoided. These results are closely confirmed in Figure 16, where we plot the steady-state composition deviation ΔX in Eq. (5) for various disturbances. Compared to the binary case (Figure 6), it is found that the temperature should be located closer to the feed stage.

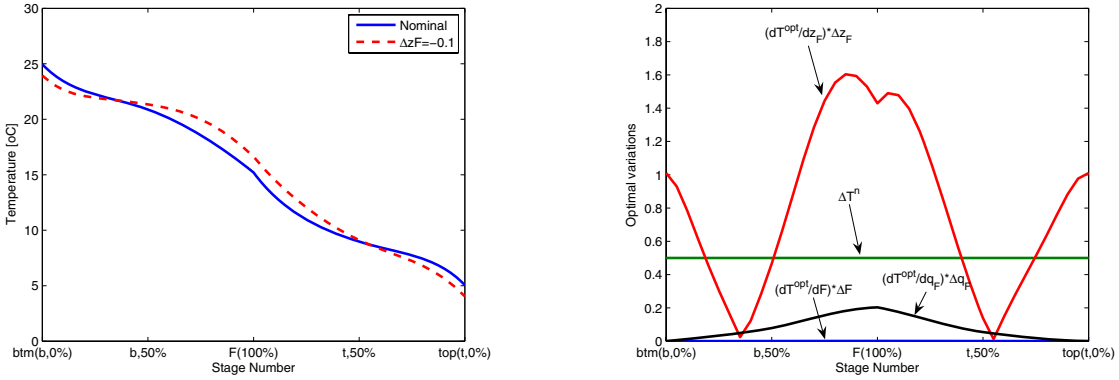

Figure 14. Re-optimized temperature profile for disturbance in z_F and resulting optimal variation for the main disturbances (multicomponent B/C separation).

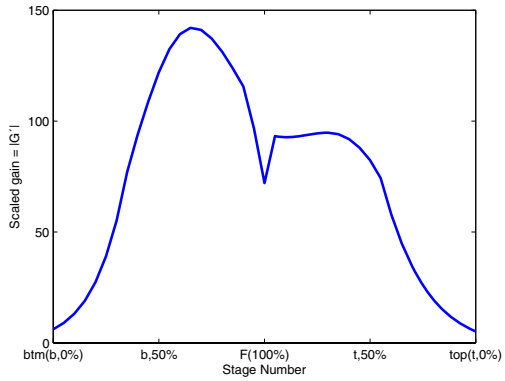

Figure 15. Multicomponent separation B/C: Scaled gain $|G'|$ computed from Eq. (4).

Results for additional control structures are presented in Table 7. The composition deviation with two optimally located temperatures ($T_{b,70\%}$ – $T_{t,75\%}$) is 1.706, which is significantly larger than 0.530 in the binary case (Table 2). This is not surprising, as temperature is generally a less reliable indication of composition for multicomponent mixtures. On the other hand, the configuration with L/F and a single temperature ($T_{b,90\%}$) has a deviation of 1.878, which is closer to the value of 0.916 for the binary case. Otherwise, the results for the multicomponent case (Table 7) are quite similar to the binary case (Table 2). The main difference is that the temperature is generally located closer to the feed stage. This is expected

as the non-key components accumulate at the end of the column (see Figure 11). The results are further confirmed by the dynamic simulations in Figure 17.

Table 7: Multicomponent separation: steady-state composition deviations.

A/B	ΔX	**B/C**	ΔX	**C/D**	ΔX
$T_{t,95\%}$ - V/B*	0.960	$T_{b,70\%}$– $T_{t,75\%}$*	1.706	$T_{b,85\%}$ – L/D*	1.373
$T_{b,80\%}$ - V/F*	1.030	**$T_{b,90\%}$ – L/F***	**1.766**	$T_{b,50\%}$ – L/D	1.469
$T_{b,80\%}$ – L/F*	**1.049**	**$T_{b,95\%}$ – L***	**1.878**	**$T_{b,40\%}$ – L/F***	**1.630**
$T_{b,80\%}$ – V*	1.066	$T_{b,75\%}$ – L/D*	1.911	$T_{b,50\%}$ – L/F	1.635
$T_{b,75\%}$ – L*	**1.075**	$T_{b,95\%}$ - V/F*	2.029	$T_{b,45\%}$ – L*	1.883
$T_{t,50\%}$ – V/B	1.272	$T_{b,50\%}$ – L/F	2.107	$T_{b,40\%}$ - V/F*	2.073
$T_{t,95\%}$ – V/F**	1.278	$T_{b,50\%}$ – L/D	2.136	$T_{b,50\%}$ – V/F	2.079
$T_{t,50\%}$ – V/F	1.376	$T_{t,95\%}$ - V/F**	2.214	$T_{t,90\%}$ - V/F**	2.215
$T_{t,50\%}$ – L/F	1.415	$T_{b,95\%}$ – V*	2.252	$T_{b,95\%}$ – $T_{t,75\%}$*	2.260
$T_{t,95\%}$ – V**	1.427	$T_{b,50\%}$ – L	2.286	$T_{t,90\%}$ – V*	2.284
$T_{t,50\%}$ - V	1.525	$T_{b,50\%}$ – V/F	2.322	$T_{b,50\%}$ - V	2.510
$T_{t,50\%}$ - L	1.538	$T_{b,50\%}$– $T_{t,50\%}$	2.530	$T_{t,50\%}$ – L/D	4.268
$T_{b,80\%}$ – $T_{t,100\%}$*	1.859	$T_{t,90\%}$ – V/B*	2.601	$T_{t,50\%}$ – L/F	4.283
$T_{b,50\%}$ – V/F	1.980	$T_{b,50\%}$ - V	2.606	$T_{t,50\%}$ - L	4.333
$T_{b,50\%}$ – L/F	1.982	$T_{b,50\%}$ – V/B	3.202	$T_{t,80\%}$ – V/B*	4.445
$T_{b,50\%}$ – V/B	1.986	$T_{t,50\%}$ – L/F	3.390	$T_{t,50\%}$ - V	4.480
$T_{b,65\%}$ – L/D*	1.999	$T_{t,50\%}$ – V/F	3.452	$T_{t,50\%}$ – V/F	4.698
$T_{b,50\%}$ – L	2.001	$T_{t,50\%}$ - L	3.556	$T_{b,50\%}$ – $T_{t,50\%}$	4.699
$T_{b,50\%}$ - V	2.002	$T_{t,50\%}$ - V	3.729	$T_{b,50\%}$ – V/B	5.278
$T_{b,50\%}$ – L/D	2.357	$T_{t,50\%}$ – L/D	3.808	$T_{t,50\%}$ – V/B	5.577
$T_{t,50\%}$ – L/D	2.543	$T_{t,50\%}$ – V/B	3.831	L/D – V/B	31.80
L/D – V/B	30.27	L/D – V/B	31.97		
$T_{b,50\%}$ – $T_{t,50\%}$	34.35	L/F – V/B	36.50		
L/F – V/B	44.66	L – B	42.81		
		D – V	43.08		
		L/D – V	46.61		
		L – V	92.03		
		L/F – V/F	123.1		

* Temperature optimally located
** Temperature optimally located in the other section

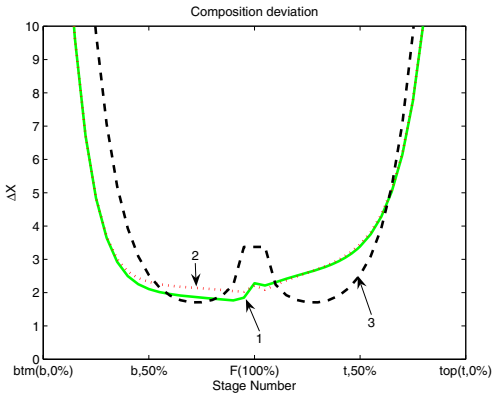

Figure 16. Composition deviation (ΔX) for fixing temperature at different locations (B/C separation): (1) L/F and one temperature. (2) V/F and one temperature. (3) Two symmetrically located temperatures.

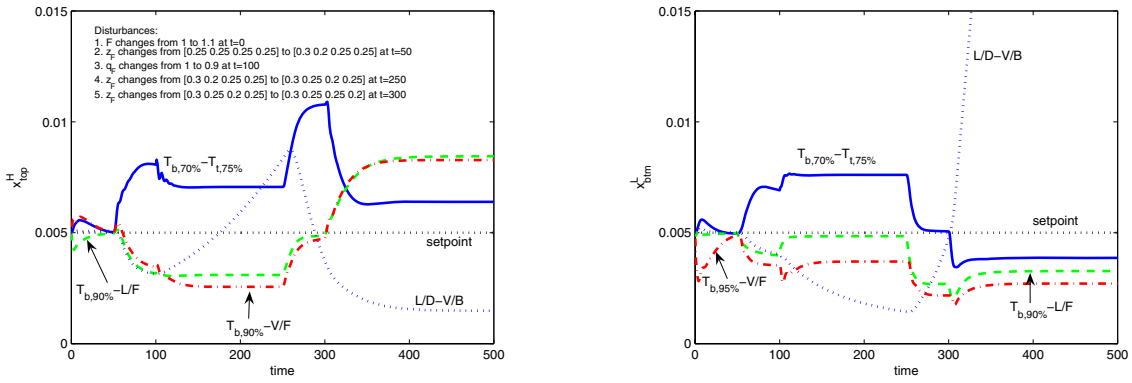

Figure 17. Multicomponent separation B/C for column A.

4.2. A/B and C/D separations

In Table 7 is shown similar results for the two other multicomponent separations (A/B and C/D separations). Interestingly, in these cases, control of two temperatures is not the best because of the influence of non-key components. For the A/B separation, with no non-keys in the top, fixing reflux L and $T_{b,75\%}$ (in the bottom towards the feed) has a deviation ΔX 1.075 whereas the best two temperatures has $\Delta X=1.859$. For the C/D separation, with no non-keys in the bottom, the best is to control a temperature in the upper part of the bottom section ($T_{b,85\%}$) and L/D, with $\Delta X=1.373$, whereas the best two temperatures has $\Delta X=2.260$.

In Figure 18 we show the temperature profiles for the multicomponent separations along with good temperature locations for each column (cross) with fixed L or L/F. Note that the temperature slope is not necessary at its maximum, and this may be explained because one should not control temperature at a location where the non-key components have a large effect on temperature. From Figure 11, we note that the heavy non-key component separates close to the bottom and just above the feed, whereas the light non-key component separates close to the top and just below the feed. Based on this insight, we state the following rule: *Locate the controlled temperature where the temperature slope is large, but (for multicomponent mixtures):*

1. If heavy non-key components: Avoid close to bottom and just above feed

2. If light non-key components: Avoid close to top and just below feed.

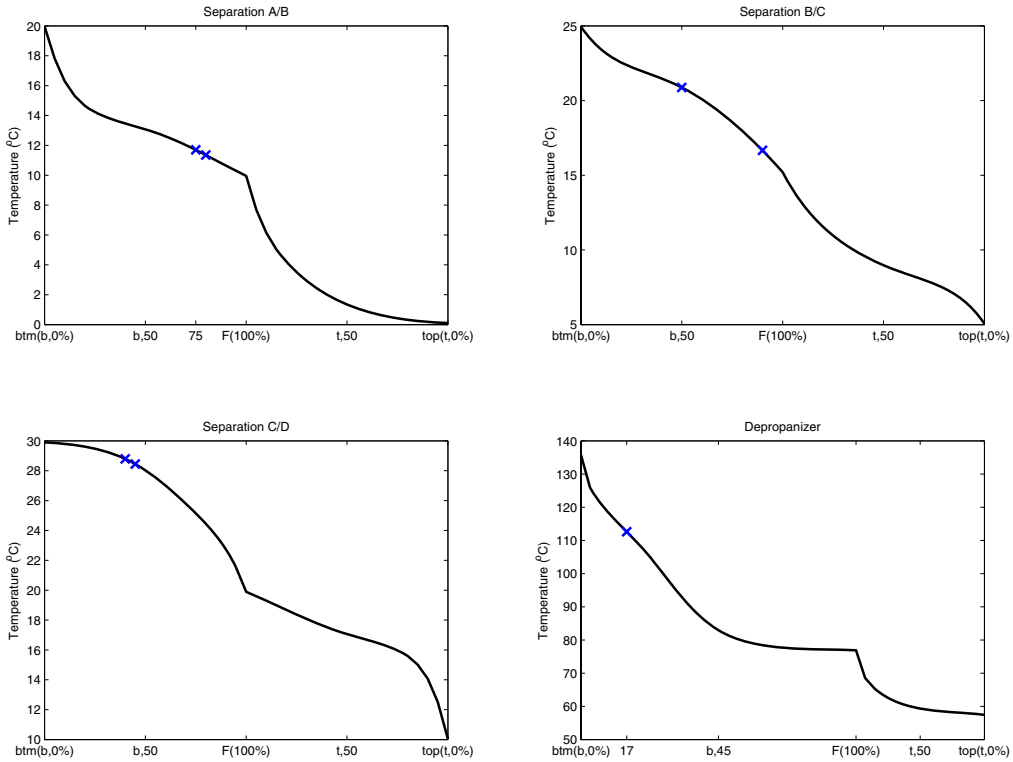

Figure 18. Temperature profiles for multicomponent separations A/B, B/C, C/D and depropanizer (line) and good temperature locations with fixed L or L/F (cross).

4.3. Depropanizer column

The above results are based on idealized mixtures with constant relative volatility, and assuming constant molar flows. However, similar results (see Table 8) have been obtained for a depropanizer case study, which has 7 components (C_2, C_3 (L), i-C_4 (H), n-C_4, i-C_5, n-C_5, n-C_6). This process was modeled in ASPEN using mass flows and SRK thermodynamics. The column has 45 stages (including reboiler and condenser) and the feed is on stage 15 (ASPEN numbers the stages from top to bottom). The mass fractions of the feed are: C_2 (0.001), C_3 (0.345), i-C_4 (0.068), n-C_4 (0.219), i-C_5 (0.085), n-C_5 (0.123), and n-C_6 (0.159). The objective of this column is to separate the propane (L = C_3) from the butane (H = i-C_4). The impurity of propane in the bottom is 0.005 and the impurity of isobutane (i-C_4) in the distillate is 0.003. Figure 19 shows the temperature profile (left) and the resulting temperature slope (solid right) together with the steady-state gain (dashed right). Note that there is no relation between the temperature slope and

the steady-state gain. From the steady-state gain, a temperature in the bottom section is preferred. This is confirmed by the steady-state composition deviations ΔX in Table 8. We find, similar to the B/C separation in the ideal multicomponent case, that the smallest composition loss is obtained using two-temperatures (ΔX=1.312) or a constant V and temperature in the middle of the bottom selection (ΔX=1.387).

The mixture contains heavy non-key components (C_5 and C_6), so from the rule just stated, one should avoid placing the temperature close to the bottom or just above the feed. Looking at the temperature profile in Figure 19a, it then seems reasonably to control temperature in the bottom section at about $T_{b,30\%}$ (at the intermediate maximum in Figure 19b). This agrees reasonably well with the deviation ΔX although it was found to be optimal to move the measurement close to the bottom at $T_{b,17\%}$.

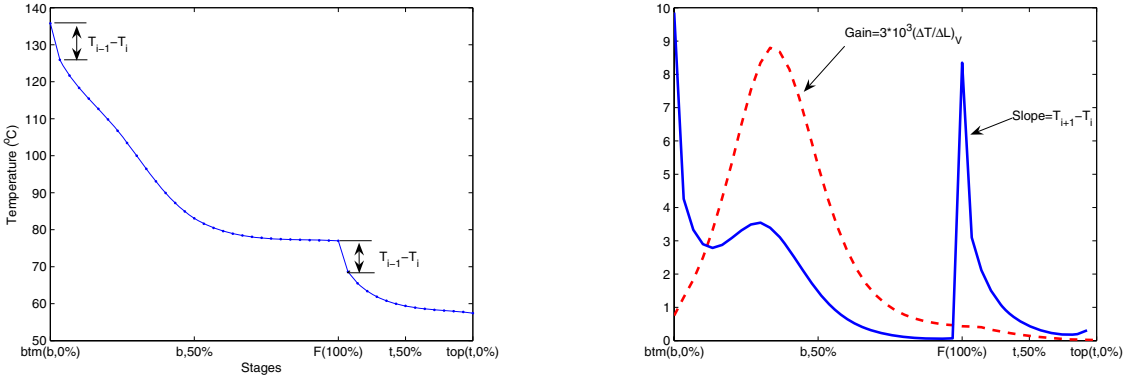

(a) (b)

Figure 19. Multicomponent depropanizer: (a) temperature profile, and (b) comparison of steady-state gain ($\left|\Delta T / \Delta L\right|$) (solid) and temperature slope ($\Delta T / \Delta N$).

Table 8: Depropanizer column: steady state composition deviations.

Fixed variables	ΔX
$T_{b,20\%} - T_{t,43\%}$*	1.312
$T_{b,20\%} - V$*	1.387
$T_{b,17\%} - L$*	**1.516**
$T_{b,17\%} - L/F$*	**1.580**
$T_{b,17\%}$ - V/F*	1.580
$T_{b,17\%}$ - V/B*	1.900
$T_{b,10\%} - L/D$*	2.744
$T_{b,50\%} - T_{t,50\%}$	3.838
$T_{t,93\%} - V/B$**	5.613
$T_{t,50\%} - V$**	6.197
$T_{t,50\%} - V/F$**	8.079

* Temperature optimally located
** Temperature optimally located in the other section

6. Conclusions

1. Overall, for binary and multicomponent separations, a good control structure for "indirect composition control" is to fix reflux L (or L/F) and a single temperature. The temperature location should be at the most sensitive stage (maximize scaled gain). This result is not new, but has here been confirmed by a systematic study. With reflux L fixed, the temperature is normally controlled by adjusting the boilup V, but if this has poor dynamic properties then a structure with fixed V and T may be used.

2. For both binary and multicomponent mixtures, the temperature sensor should be located away from the column ends, especially for column ends with high purity (in terms of the key components).

3. A common heuristic is to select a temperature where the change in temperature from tray to tray ("slope") is the largest (steep temperature profile) (Luyben, 2005). The heuristic is correct for the dynamic response (see Appendix), and is confirmed at steady-state for binary mixtures. However, for multicomponent mixtures the rule needs to be modified to avoid the effect of non-key components on the temperature:

1. If heavy non-key components: Avoid close to bottom and just above feed
2. If light non-key components: Avoid close to top and just below feed.

4. Control of two temperatures is better for some columns, but a simple rule for when it is better has not been found.

5. Note that the results in this paper are for steady state and are independent of how we do the level control. For example, it is possible to use L for condenser level control, and then adjust D at a slower time scale to "reset" L to a desired steady-state value. Also note that with good indirect composition control, we get less variation in levels because we avoid redistribution of components in the column.

Appendix: Temperature slope and dynamics response

A commonly used heuristic is to control the temperature at the location where the temperature slope (temperature difference between neighboring stages) is large (e.g., Luyben, 2005). This makes sense from a dynamic point of view because the initial (high frequency) gain is directly proportional to the temperature difference. The objective of this Appendix is to prove this: To this effect, note that the initial change in the mole fraction $x(j)$ of any component j in response to a step change in reflux (ΔL_i) and boilup (ΔV_i) is (Eq. 65 in Skogestad, 1997):

$$t = 0^+ : \qquad \frac{\mathrm{d}x_i(j)}{\mathrm{d}t} = \frac{1}{M_i}\left(\bar{x}_{i+1}(j) - \bar{x}_i(j)\right)\left(\Delta L_i - \frac{\bar{L}_i}{\bar{V}_i}\Delta V_i\right) \tag{11}$$

where *i* denotes stage number, M_i the stage holdup and bar(-) denotes steady-state values.

Multiplying the equation for each component x(j) by its boiling point $T_b(j)$, summing the equations and introducing the simplified temperature expression $T_i = \sum_j T_b(j)x_i(j)$ gives an expression for the temperature on stage *i*:

$$t = 0^+ : \qquad \frac{\mathrm{d}T_i}{\mathrm{d}t} = \frac{1}{M_i}\left(\bar{T}_{i+1} - \bar{T}_i\right)\left(\Delta L_i - \frac{\bar{L}_i}{\bar{V}_i}\Delta V_i\right) \tag{12}$$

We see that the "initial" gain ($\mathrm{d}T_j/\mathrm{d}t$) from ΔL_i and ΔV_i to T_i is proportional with the difference in temperature $\left(\bar{T}_{i+1} - \bar{T}_i\right)$ from one stage to the next. For dynamic control purpose we prefer a large dynamic gain (e.g., to avoid an initial effective delay, input saturation and sensitivity to measurement noise) and it is then good to control temperature at a stage where the slope is large, or at least to avoid a location where the slope is small (avoid constant temperature regions).

Acknowledgements

Comments from Dr. Muhammad Al-Arfaj are gratefully acknowledged.

Nomenclature

B – bottom product [kmol/min]

c – secondary controlled variables

D – distillate (top product) [kmol/min]

F – feed rate [kmol/min]

G – transfer matrix

H – heavy key-component

J – objective function

L – reflux flow rate [kmol/min] or light key-component

N – number of theorical stages in column (including reboiler and condenser)

q_F – fraction liquid in feed

T_b - temperature located in bottom section

T_t - temperature located in top section

$T_{B,H}$ –boiling temperature

V – boilup from reboiler [kmol/min]

x_{btm}^{L} – mole fraction of light component in bottom product

x_{top}^{H} - mole fraction of light component in distillate (top product)

z_F - mole fraction of light component in feed

Greek letters

α - relative volatility

ΔF - expected disturbance in feed flowrate

Δq_F - expected disturbance in feed enthalpy

ΔX - composition deviation (see Eq. 1)

Δz_F - expected disturbance in feed composition

θ_m – composition measurement delay [min]

References

Halvorsen, I.J., Skogestad, S., Morud, J. and Alstad, V., 2003, Optimal selection of controlled variables. *Ind Eng Chem Res*, 42: 3273-3284.

Luyben, W.L., 1975, Steady-state energy-conservation aspects of distillation control system design. *Ind Eng Chem Fundam*, 14(4):321-325.

Luyben, W.L., 2005, Effect of feed composition on the selection of control structures for high-purity binary distillation. *Ind Eng Chem Res*, 44: 7800-7813.

Luyben, W. L., 2006, Evaluation of criteria for selecting temperature control trays in distillation columns, *J. Proc. Control*, 16: 115-134.

Moore, C.F., 1992, Selection of controlled and manipulated variables, in *Practical Distillation Control*, Luyben, W.L. (ed.) (Van Nostrand Reinhold: New York), pp 140-177.

Shinskey, F.G., 1984, Distillation Control 2nd Edition (McGraw-Hill).

Skogestad, S., 1997, Dynamics and control of distillation columns: a tutorial introduction. *Trans IChemE*, 75(A6): 539-562.

Skogestad, S., 2000, Plantwide control: the search for the self-optimizing control structure. *J Proc Cont*, 10(5): 487-507.

Skogestad, S., 2003, Simple rules for model reduction and PID controller tuning. *J Proc Cont*, 23: 291-309.

Skogestad, S., Lundström, P., Jacobsen, E.W., 1990, Selecting the best distillation control configuration, *Aiche J.*, 36(5):753-764.

Tolliver, T.L. and McCune L.C., 1980, Finding the optimum temperature control trays for distillation-columns. *Instrum Tech*, 27(9): 75-80.

Figure Captions:

Figure 1. Distillation column with fixed reflux L and temperature control in the bottom section.

Figure 2. Binary column A: Temperature profile resulting from change in reflux (L) with fixed V (left) and resulting steady-state gain $\left|\Delta T / \Delta L\right|$ for small ΔL (right).

Figure 3. Binary column A: (a) temperature profile, and (b) resulting temperature slope ($\Delta T / \Delta N$).

Figure 4. Binary column A: Re-optimized temperature profile for disturbance in z_F (left) and resulting optimal variation for the main disturbances (right).

Figure 5. Binary column A: Scaled gain $\left|G'\right|$ computed from Eq. (4).

Figure 6. Binary column A: Composition deviation (ΔX) for fixing temperature at different locations: (1) L/F and one temperature. (2) V/F and one temperature. (3) Two symmetrically located temperatures.

Figure 7. Dynamic composition response for alternative structure without explicit composition control (Binary Column A). Disturbances: F from 1 to 1.1 (t = 0); q_F from 1 to 0.9 (t = 40 min); and z_F from 0.5 to 0.55 (t = 60 min).

Figure 8. Dynamic response with composition layer ($\theta_m = 10$ min) – Binary column A. Disturbances: F from 1 to 1.1 (t = 0); q_F from 1 to 0.9 (t = 250); z_F from 0.5 to 0.55 (t = 500); $x^{L}_{btm,s}$ from 0.01 to 0.011 (t = 750); and $x^{H}_{top,s}$ from 0.01 to 0.011 (t = 1000).

Figure 9. Temperature profiles for binary columns A-J with crosses to indicate good temperature locations with fixed L or L/F.

Figure 10. Temperature profiles for binary columns M1-M6 with cross to indicate good temperature locations with fixed L or L/F.

Figure 11. Steady state composition profile for B/C separation in multicomponent column A.

Figure 12. Temperature profile resulting from change in reflux (L) with fixed V and resulting steady-state gain ($\Delta T_i / \Delta L$) (multicomponent B/C separation).

Figure 13. Nominal optimal temperature profile and resulted temperature slope $\Delta T / \Delta N$ for multicomponent B/C separation.

Figure 14. Re-optimized temperature profile for disturbance in z_F and resulting optimal variation for the main disturbances (multicomponent B/C separation).

Figure 15. Multicomponent separation B/C: Scaled gain $\left|G'\right|$ computed from Eq. (4).

Figure 16. Composition deviation (ΔX) for fixing temperature at different locations (B/C separation): (1) L/F and one temperature. (2) V/F and one temperature. (3) Two symmetrically located temperatures.

Figure 17. Multicomponent separation B/C for column A.

Figure 18. Temperature profiles for multicomponent separations A/B, B/C, C/D and depropanizer (line) and good temperature locations with fixed L or L/F (cross).

Figure 19. Multicomponent depropanizer: (a) temperature profile, and (b) comparison of steady-state gain ($\left|\Delta T / \Delta L\right|$) (solid) and temperature slope ($\Delta T / \Delta N$).